Impact of Emitter Electron Launcher on the Performance of Type-II InP/GaAsSb DHBTs

Mojtaba Ebrahimi, Sara Hamzeloui, Akshay M. Arabhavi, Filippo Ciabattini, Andrea Cercaci, Olivier Ostinelli, and Colombo R. Bolognesi *Fellow, IEEE*

Millimeter-Wave Electronics (MWE) Group, ETH-Zurich, Gloriastrasse 35, 8092 Zurich, Switzerland

mebrahimi@mwe.ee.ethz.ch, colombo@ieee.org

***Abstract*— This work investigates the impact of an emitter electron launcher on the DC and RF performance of Type-II InP/GaAsSb double heterojunction bipolar transistors (DHBTs). The introduction of the electron launcher results in improved DC characteristics, including an improved base current ideality factor and an increased common-emitter current gain, β. The improved ideality factor indicates suppressed recombination current, leading to enhanced electron injection efficiency into the base. Statistical analysis further confirms reduced emitter-size dependence and improved β uniformity, with an overall increase of approximately 30% compared to a reference standard DHBT. RF measurements show no significant degradation, with only a slight reduction in f_T, particularly for narrow devices, attributed to increased emitter resistance due to higher Ga content. These results demonstrate that the emitter electron launcher is an effective approach for improving DC performance while maintaining RF characteristics, offering potential for further device scaling and optimization.**

***Keywords*— Double heterojunction bipolar transistors (DHBTs), modified double heterojunction bipolar transistors (mDHBTs), GaAsSb, InP, Breakdown, THz.**

I. Introduction

Double heterojunction bipolar transistors (DHBTs) based on the Type-II InP/GaAsSb material system have attracted significant attention for high-speed and high-frequency applications due to their favorable band alignment and excellent transport properties [1]. In particular, these devices offer high breakdown voltage and competitive RF performance, making them strong candidates for next-generation millimeter-wave and terahertz technologies [2]. However, further performance improvements are often limited by recombination currents in the base-emitter junction, which degrade the base current ideality factor and reduce the common-emitter current gain, β.

Various approaches have been proposed to enhance carrier injection efficiency and suppress recombination mechanisms in DHBTs. Among these, the incorporation of an emitter electron launcher has emerged as a promising technique to improve electron injection into the base by engineering the emitter energy profile. By modifying the emitter composition, particularly through increased Ga content, the electron launcher can effectively reduce the recombination component of the base current, leading to improved DC performance. Increasing the Ga content of the GaInP composition results in a larger ΔE_C [3]. This can be increased in the GaInP emitter to further accelerate electrons by creating a larger energy ramp at the emitter–base junction. However, this is limited by lattice mismatch and strain between GaInP and GaAsSb.

Despite these advantages, the impact of such design modifications on RF performance remains a critical concern. Changes in emitter composition may introduce increased emitter resistance, which can potentially degrade high-frequency figures-of-merit such as the cutoff frequency, f_T, and the maximum oscillation frequency, f_{MAX}. Therefore, a comprehensive evaluation of both DC and RF characteristics is essential to assess the overall benefit of the emitter electron launcher concept.

In this work, the effect of an emitter electron launcher on the performance of Type-II InP/GaAsSb DHBTs is investigated. Devices with identical geometries are compared to a reference structure to isolate the influence of the emitter design. Both DC and RF measurements, along with statistical analysis across device sizes, are presented to evaluate improvements in gain, ideality factor, and scalability. The results demonstrate enhanced DC performance with minimal impact on RF characteristics, highlighting the potential of the emitter electron launcher for future high-speed device optimization.

II. Device Fabrication

DHBT epitaxial layers differing only in emitter composition were grown by metal-organic chemical vapor deposition (MOCVD) on 2-inch semi-insulating InP substrates. The details of the epilayers are given in Table 1. DHBTs with the $Ga_{0.22}In_{0.78}P/GaAs_{0.59}Sb_{0.41}$ (DHBT1) and $Ga_{0.27}In_{0.73}P/GaAs_{0.59}Sb_{0.41}$ (DHBT2) emitter/base interface layers were successfully fabricated. The two structures differ in the emitter composition adjacent to the base layer: $Ga_{0.22}In_{0.78}P/GaAs_{0.59}Sb_{0.41}$ (DHBT1) and $Ga_{0.27}In_{0.73}P/GaAs_{0.59}Sb_{0.41}$ (DHBT2). In both cases, the emitter consists of 15 nm $Ga_yIn_{1-y}P$, where the first 5 nm adjacent to the base have a constant composition, followed by a 10 nm region that is linearly graded to $y = 0$. The intermediate n^+ InP layer and the GaInAs cap are doped at concentrations of $\sim 1.5 \times 10^{19}$ cm^{-3} and $\sim 3.8 \times 10^{19}$ cm^{-3}, respectively. The transistors feature a 20-nm-thick $GaAs_xSb_{1-x}$ base with a

Table 1. Epitaxial Layer Structure

	Material	Doping [cm^{-3}]	Thickness [nm]
Emitter Contact	$Ga_{0.25}In_{0.75}As$	Si: 3.8E19	5
	$Ga_{0.47}In_{0.53}As$ → $Ga_{0.25}In_{0.75}As$	Si: 3.8E19	10
	$Ga_{0.47}In_{0.53}As$	Si: 3.8E19	20
Emitter (DHBT1)	InP	Si: 1.5E19	130
	InP	Si: 2.2E19	5
	$Ga_{0.22}In_{0.78}P$ → InP	**Si: 2.2E16**	**10**
	$Ga_{0.22}In_{0.78}P$	**Si: 2.2E16**	**5**
Emitter (DHBT2)	InP	Si: 1.5E19	130
	InP	Si: 2.2E19	5
	$Ga_{0.27}In_{0.73}P$ → InP	**Si: 2.2E16**	**10**
	$Ga_{0.27}In_{0.73}P$	**Si: 2.2E16**	**5**
Base	$GaAs_{0.41}Sb_{0.59}$ → $GaAs_{0.59}Sb_{0.41}$	C: 8.5E19	20
Collector	InP	Si: 9.4E16	125
Sub-Collector	InP	S: 3.1E19	50
Collector Contact	$Ga_{0.47}In_{0.53}As$	Si: 3.0E19	20
Buffer	InP	S: 2.8E19	300
Substrate	InP	Semi-insulating	350000

sheet resistance of $R_{SH} \approx 1140\,\Omega/\square$ and an average doping concentration of $N_{B,\,AV} \approx 8.5 \times 10^{19}$ cm^{-3}. The InP collector, buffer, and substrate are identical for both structures. The bandgap differences ΔE_G for 27% Ga relative to the standard 22% Ga in GaInP composition is 52 meV [4].

DHBTs were fabricated side-by-side in a self-aligned triple mesa process, with the emitter and base contacts defined by electron-beam lithography. The base contact metallization employs an electron-beam–evaporated Pt/Ir/Pt/Au refractory stack to suppress metal diffusion into the base during high-temperature benzo-cyclo-butene (BCB) curing [5]. The emitter mesa sidewalls and the extrinsic base surface were passivated with atomic layer deposited (ALD) Al_2O_3. The self-aligned emitter and base mesas were formed by combined dry and wet etching, followed by photolithographic definition and electron-beam evaporation of the collector contact. After deposition of the collector contact, the devices were electrically isolated and planarized using BCB. Finally, the process was completed by depositing ground–signal–ground (GSG) probe pads.

III. Results and Discussions

A. DC Measurements

The static performance of the DHBTs was characterized using an HP4156B semiconductor parameter analyzer. The Gummel characteristics measured at $V_{CB} = 0$ V for a $(0.25 \times 7.5)\,\mu m^2$ DHBT1 and DHBT2 are shown in Fig. 2. The DC results show a reduced base current ideality factor for the new emitter design (DHBT2), along with an improved gain compared to the standard DHBT (DHBT1). The base current ideality, factor η_B, decreases from 1.38 to 1.22. The reduction in the ideality factor indicates a decrease in recombination current. Therefore, in DHBT2, electron injection into the base is enhanced, resulting in an increased common emitter current

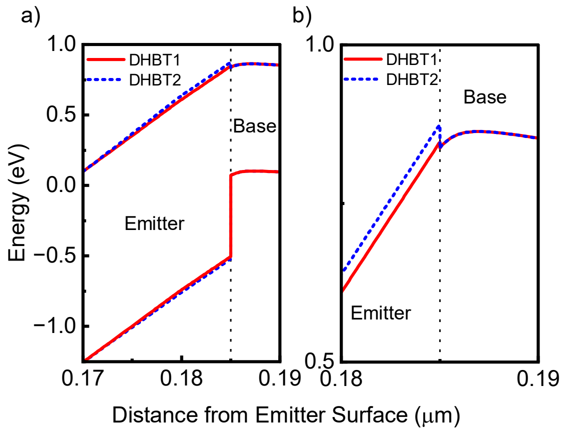

Fig. 1. a) Equilibrium band diagrams of the DHBT1 and DHBT2 at the emitter-base junction. b) Zoomed-in conduction band diagram at the emitter-base junction.

gain β from 22 to 28. The collector ideality factor remains unchanged at 1.01 for both structures.

B. Small-Signal RF Measurements

The small-signal RF performance was measured using a PNA-X vector network analyzer over the frequency range of 0.2-50 GHz with an input power of -30 dBm. An off-wafer impedance standard and LRRM (line–reflect–reflect–match) calibration were employed to establish the reference planes at the probe tips. Following conventional short–open de-embedding, Mason's unilateral power gain (U) and the common-emitter short-circuit current gain $|h_{21}|^2$ were plotted as a function of frequency, as shown in Fig. 3. Extrapolation based on single-pole fits over the full frequency range yields a peak $f_{MAX} = 745$ GHz with $f_T = 460$ GHz at $V_{CE} = 1.1$ V for the DHBT1, and a peak $f_{MAX} = 786$ GHz with $f_T = 445$ GHz at $V_{CE} = 1.1$ V for the DHBT2. The RF results show no notable difference between the two structures, with only a slight reduction in f_T and a slight increase in f_{MAX} for the DHBT2.

C. Statistical Analysis

A comprehensive statistical analysis was performed on more than 100 devices from each structure, as illustrated in Fig. 4. The results indicate that the new design mitigates emitter-size effects and yields a more stable β as a function of device size. Furthermore, the overall β is about 30% higher in DHBT2. The RF results indicate a slight decrease in f_T for DHBT2, especially for devices with narrower emitter widths. This is attributed to the higher emitter resistance in DHBT2 due to the increased Ga content in the emitter. Nevertheless, the overall RF performance, including f_{MAX}, remains largely unaffected.

IV. Conclusion

In conclusion, the incorporation of an emitter electron launcher in Type-II InP/GaAsSb DHBTs improves DC

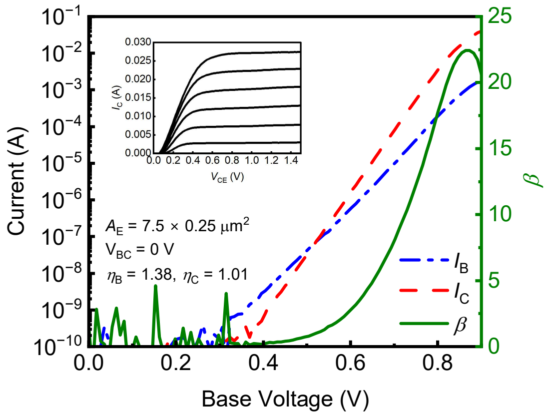

(a) DHBT1

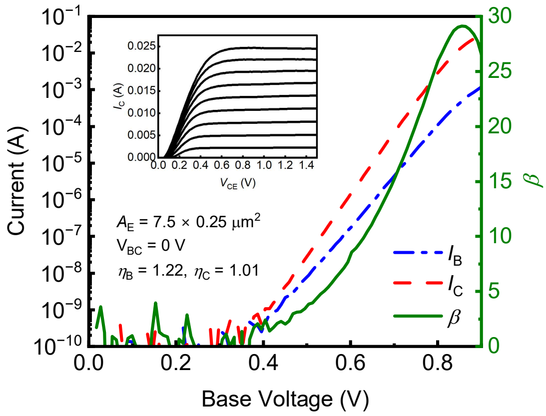

(b) DHBT2

Fig. 2. Gummel characteristics (V_{CB} = 0 V) of a $0.25 \times 7.5\,\mu m^2$ (a) DHBT and (b) mDHBT. The DC gain as a function of V_{BE} is also plotted. Inset: Corresponding common-emitter *I-V* curves.

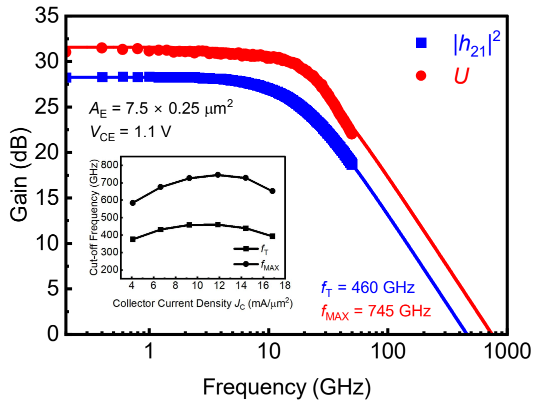

(a) DHBT1

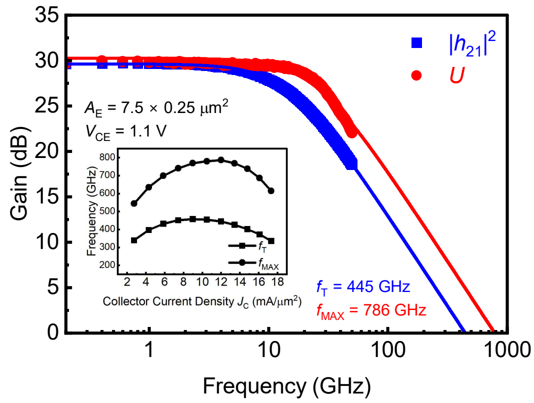

(b) DHBT2

Fig. 3. Measured small-signal current gain $|h_{21}|^2$, and Mason's unilateral gain U of (a) DHBT and (b) mDHBT. f_T and f_{MAX} are determined from single-pole fits and extrapolations. Inset: Bias dependence of f_T and f_{MAX} vs. current density.

performance while preserving RF characteristics. The new design (DHBT2) shows a reduced base current ideality factor, indicating lower recombination current and enhanced electron injection, resulting in a higher β. Statistical analysis confirms improved uniformity and reduced emitter-size dependence.

RF performance remains largely unchanged, with only a slight reduction in f_T attributed to increased emitter resistance, while f_{MAX} is unaffected. These results highlight the effectiveness of the emitter electron launcher for improving device performance and enabling further scaling.

Acknowledgment

The authors would like to thank the staff of FIRST Lab at ETH Zurich, Zurich, Switzerland, for their support.

References

[1] C. R. Bolognesi, A. M. Arabhavi, R. Hersent, S. Hamzeloui, F. Jorge, X. Wen, M. Riet, M. Luisier, V. Nodjiadjim, F. Ciabattini, C. Mismer, O. Ostinelli, and A. Konczykowska, "InP/GaAsSb DHBTs: Thz analog performance and record 180-Gb/s 5.5vppd-swing PAM-4 DAC-driver," in *2022 IEEE BiCMOS and Compound Semiconductor Integrated Circuits and Technology Symposium (BCICTS)*, 2022, pp. 112–119.

[2] A. M. Arabhavi, F. Ciabattini, S. Hamzeloui, R. Flückiger, T. Saranovac, D. Han, D. Marti, G. Bonomo, R. Chaudhary, O. Ostinelli, and C. R. Bolognesi, "InP/GaAsSb double heterojunction bipolar transistor emitter-fin technology with f_{MAX} = 1.2 THz," *IEEE Transactions on Electron Devices*, vol. 69, no. 4, pp. 2122–2129, April 2022.

[3] I. Vurgaftman, J. R. Meyer, and L. R. Ram-Mohan, "Band parameters for III-V compound semiconductors and their alloys," *Journal of Applied Physics*, vol. 89, no. 11, pp. 5815–5875, 06 2001. [Online]. Available: https://doi.org/10.1063/1.1368156

[4] A. Laugier and J. Chevallier, "About the band structure of GaxIn1-xP alloys," *Solid State Communications*, vol. 10, no. 4, pp. 353–356, 1972. [Online]. Available: https://www.sciencedirect.com/science/article/pii/0038109872904401

[5] F. Ciabattini, A. M. Arabhavi, S. Hamzeloui, G. Bonomo, M. Ebrahimi, O. Ostinelli, and C. R. Bolognesi, "High-temperature stability base ohmic contacts for InP/GaAsSb DHBTs," in *2024 IEEE BiCMOS and Compound Semiconductor Integrated Circuits and Technology Symposium (BCICTS)*, 2024, pp. 84–87.

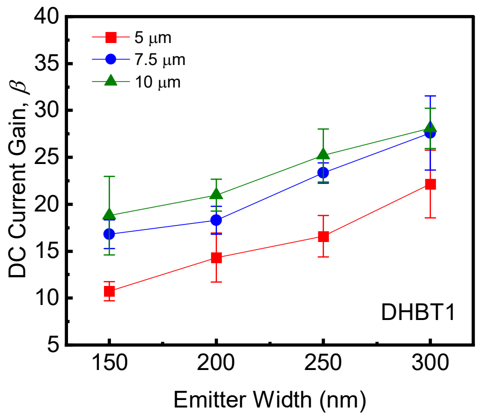

(a) β scaling behavior in DHBT1.

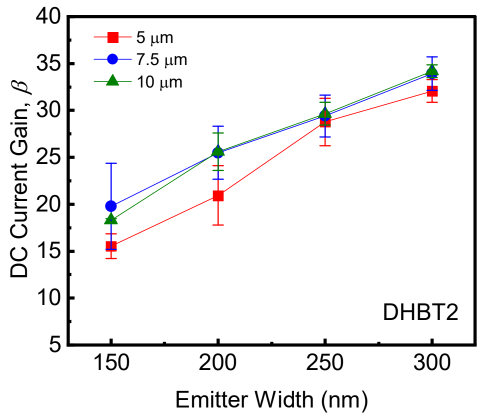

(b) β scaling behavior in DHBT2.

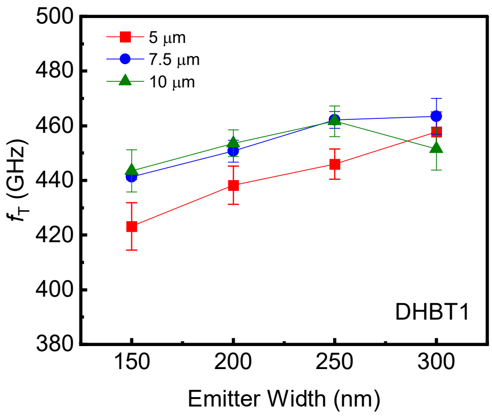

(c) f_{T} scaling behavior in DHBT1.

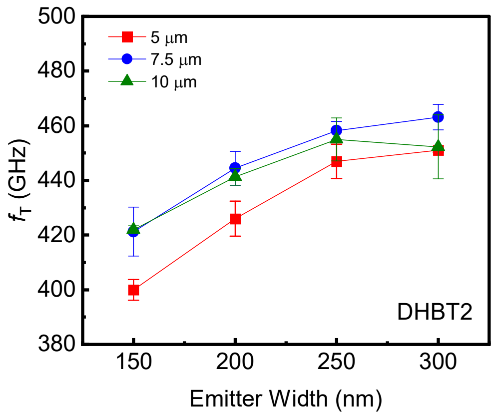

(d) f_{T} scaling behavior in DHBT2.

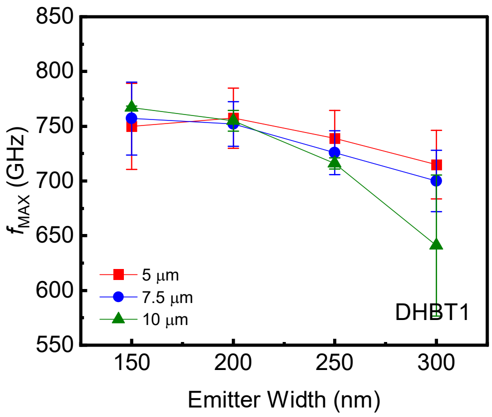

(e) f_{MAX} scaling behavior in DHBT1.

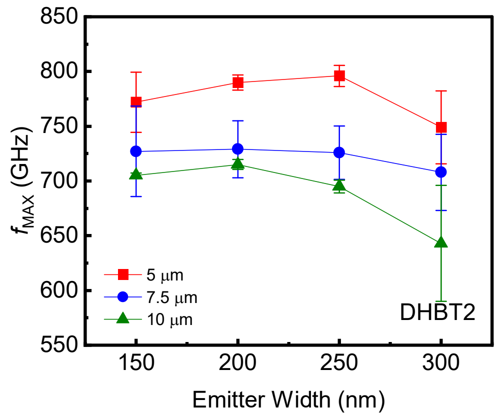

(f) f_{MAX} scaling behavior in DHBT2.

Fig. 4. Statistical analysis of DHBT1 and DHBT2.